ISSN 2349-0292
Impact Factor 3.802

GLOBAL JOURNAL OF ADVANCED ENGINEERING TECHNOLOGIES AND SCIENCES

SOUR CORROSION INHIBITION USING FACILE-DESIGNS OF SCHIFF BASE POLYMERS FOR CARBON STEEL PIPELINES

Shimaa A. Higazy [1,*], Ahmed M. Al-Sabagh [1], Adel A.-H.Abdel-Rahman [2], Notaila M. Nasser[1], Olfat E. El-Azabawy [1,*] and Eman A. Khamis [1]

[1,*]Petroleum Application Department, Egyptian Petroleum Research Institute (EPRI), Nasr City 11727, Cairo, Egypt.

[2]Chemistry Department, Faculty of Science, Menoufiya University, Menoufiya, Egypt.

DOI: 10.5281/zenodo.3263775

ABSTRACT

As an economic and applied materials, three Schiff base polymers which have the structure of -CH=N- double bond were synthesized by facile polycondensation reactions and applied as corrosion inhibitors in sour media. Because of their enhanced film-forming ability and multifunctionality, poly Schiff bases possess higher protective barrier features than other corrosion inhibitors. FTIR, ^{1}HNMR, GPC, and TGA were used to characterize the as-synthesized polymers. These polymers are efficient and economic corrosion inhibitors for sour media. Polarization resistance method was used to test the corrosion rate mode, where the electrochemical impedance spectroscopy (EIS) was investigated. Field emission SEM and EDX were used to investigate the morphology of corrosion and surface composition of carbon steel samples. These outstanding poly Schiff base materials demonstrated a high corrosion inhibition, and are therefore recommended as a guide for the design of inhibitor in sour condition. The electronic structures and molecular geometry were investigated through quantum calculations which indicated the chemical reactivity and kinetic stability of compounds. The PSB2 presented the most profound sour corrosion inhibition properties when tested through electrochemical techniques. Its 300 ppm dosage yielded 90.21 % and 86.19 % inhibition efficiencies in potentiodynamic polarization and EIS measurements, respectively.

Keywords: Schiff base polymers; Sour corrosive media; Corrosion inhibitors; Polarization resistance; SEM; Quantum calculations.

INTRODUCTION

Oil field industry represents an essential section in industrial applications [1]. Among various applicable alloys in the industry, carbon steels represent a cost-effective material with high strength which makes carbon steel pipes an ideal choice for numerous industrial applications [2]. As a result, studying the corrosion of carbon steel is essential in different petrochemical applications [3,4]. Some impurities such as H_2S, H_2O, CO_2 and O_2, bacterial and organic acids are included which negatively affect the carbon steel corrosion [5,6]. However, H_2S exhibited higher water solubility and corrosion impacts than many impurities particularly CO_2 and O_2 at atmospheric temperature and pressure [7]. In sour wells, hydrogen sulfide is the primary corrosive agent [8]. Pitting corrosion on a carbon steel surface is produced by H_2S through the formation of iron sulfide. Severe corrosion in petroleum fields is caused by H_2S impurities, which form a molecular surface complex even exist at ppm levels [9,10]. The complex can yield hydrogen atoms which recombine to form molecular gases hydrogen; whereas some can diffuse in the carbon steel and cause surface blistering or cracking [11]. Surface science is greatly concerned with the organic inhibitor's adsorption, which alters the metal corrosion resistance [12]. An ultra-thin anticorrosion layer composed of metal-inhibitor complex can create a barrier between the metal and the corrosive media through interaction of the polymeric inhibitor with the ionic Fe^{2+} on the surface [13,14]. Organic compounds including nitrogen and other heteroatoms are widely applicable as corrosion inhibitors [15]. Organic polymers, especially Schiff base polymers, possess eco-friendly properties and excellent corrosion inhibition, so modern researches were directed toward their applications to resist the corrosion in the petroleum industry [16]. Poly Schiff base (PSB) is formed by polycondensation of diamine with dialdehyde or diketone to form imine (-CH=N-) groups.

Through a chemical and/or physical adsorption mechanism, these polymers with the imine groups are filmed on the steel surface, which cause higher inhibition ability than those containing -NH_2, -CHO and/or C=O groups. Double bond electron donations of the imine group as well as the nitrogen lone pair of electrons cause high corrosion inhibition [17]. These polymers with polar nitrogen atoms and high solubility exhibit stabilized

corrosion inhibition [18]. In the present work, we prepared three new Schiff base polymers via polycondensation technique. The three polymers were applied as corrosion inhibitors in sour petroleum condition for protecting pipeline carbon steel. These polymers are dissolved in formation water under sour condition to be tested as corrosion inhibitors. To the best of our knowledge, this is the first work to synthesis these polymers and investigates their anticorrosion activity in the sour petroleum environment; where different polymers and H_2S concentrations were used to study the anticorrosion performance of carbon steel. It was inevitable to study the open-circuit potential, electrochemical impedance spectroscopy as well as the potentiodynamic polarizations electrochemical tests. These tests were performed using (0, 20, 50, 100, 300 and 500 ppm (mmol/L)) concentrations of inhibitors dispersed in formation water. The anticorrosion performance of these inhibitors towards carbon steel was also assessed at different concentrations of H_2S. Field emission scanning electron microscope (FESEM) studied the morphology of the carbon steel sample surface after exposure to sour media with and without inhibitors, while the energy dispersive x-ray (EDX) analyzed their surface chemical composition. The obtained results confirmed the high corrosion inhibition of the prepared polymers in the sour petroleum environment. The current work introduces several merits, such as facility, ecological and economic impacts, and powerful applications for carbon steel protection against corrosion.

MATERIALS AND METHODS

Materials

1,3-diaminopropane ($(CH_2)_3(NH_2)_2$, 99%) and 1,7-diaminoheptane ($(CH_2)_7(NH_2)_2$, 98%) were delivered from Acros Company (Belgium). Glutaraldehyde solution (50 wt. % in H_2O), sodium sulfide (Na_2S, extra pure), hydrochloric acid (HCL, 37%) and 1,12-diaminododecane ($(NH_2(CH_2)_{12}NH_2$, 98%) were obtained from Sigma–Aldrich Company Ltd. Ethanol (AR) and acetone (HPLC) were purchased from Fischer Company (UK).

Synthesis of poly Schiff bases (PSB1, PSB2 and PSB3)

The PSB1 (Scheme 1a) was prepared by a polycondensation reaction of glutaraldehyde with 1,3-diaminopropane. The reaction was performed in a three neck round-bottomed flask fitted with a condenser, a thermometer and an arrangement containing nitrogen inlet and outlet. In brief, the flask was supplied with 81.03 g of glutaraldehyde and 60 mL ethanol. Then, 1,3-diaminopropane (30 g) was dropwisely introduced and the temperature was gradually raised up to 85 ˚C for 12-hour stirring. Molar ratio of glutaraldehyde and 1,3-diaminopropane was (1:1 mole). The viscosity of the material was tremendously increased with reaction time. Then the temperature was lowered gradually to room temperature with stirring. The solvent was removed and the polymer was purified by vacuum distillation.

The PSB2 (Scheme 1b) was also prepared via a polycondensation reaction between glutaraldehyde and 1,7-diaminoheptane as follow: To a solution of glutaraldehyde (9.26 g) in an acidic solution, 1,7-diaminoheptane (6.02 g) was added drop by drop to the mixture and stirred for 12 h at 105°±5 °C. A rotary evaporator was used to evaporate and dry the yielded precipitate. The PSB3 (Scheme 1c) was synthesized via a polycondensation between glutaraldehyde and 1,12-diaminododecanewith 1:1 molar ratio of the reactants as mentioned before.

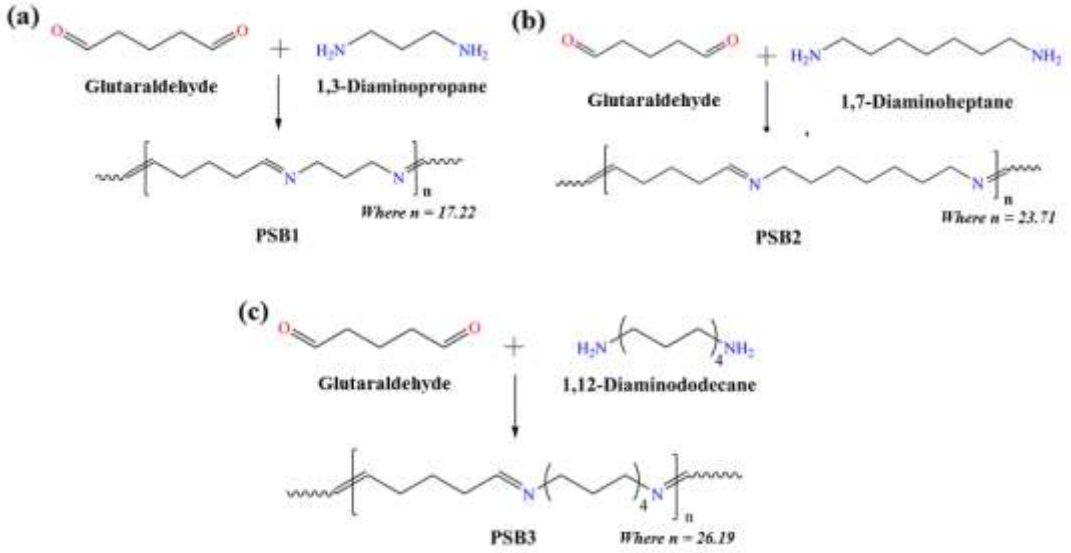

Scheme 1: The Synthesis of (a) PSB1, (b) PSB2, and (c) PSB3 via polycondensation reaction

ISSN 2349-0292
Impact Factor 3.802

Characterization techniques

A Nicolet™iS™10 (Thermo Fisher scientific, USA) instrument and KBr pellets (Scharlau, Spain) were used for the FTIR analysis; which employed within 400–4000 cm^{-1} range of scan using Thermo Scientific OMNIC TM Software. An Avance 400 MHz spectrometer (Bruker, Germany) was used for ^{1}HNMR. The polymers were dissolved by CDCl3, while the internal standard was tetramethyl silane. GPC analysis was used to determine the distributions of the polymers' molecular weights through PL-GPC-220, Agilent Technologies, United States. The system was equipped with three columns PlgelOlexis (300 × 7,5 mm) using tetrahydrofuran (THF) as a solvent and the calibration of refractive index detector occurred through a standard of polystyrene and a universal mode. Discovery TGA-55 (TA instrument, United States) was used to study the polymeric thermal stability. The specimen was scanned at 25°C–800°C under nitrogen with rate 10°C/min.

Sample preparation and the corrosion media

A working electrodemade of carbon steel rod sample with ((weight %) of C 0.097, Si 0.032, Mn 0.439, P 0.013, S 0.018, Cr 0.026, Mo 0.002, Ni 0.001, Al 0.002, Co 0.0005, Cu 0.018, V 0.0008 and the rest is Fe) chemical composition was used for the anticorrosion evaluations using PSBs inhibitors. This electrode was embedded in a Teflon holder with an exposed (1 cm^2) cross-section of the rod sample. Emery papers with various grades (600-1200) were used to polish the electrodes before every test; acetone and distilled H_2O were used for washing and then dried with warm air. Oil well formation water used herein as the corrosive solution was supplied by a petroleum company (Badr El Din, Egypt). Table 1 elucidated its chemical composition and physical characteristics. Herein, 100 ppm of H_2S were produced in the solution in-situ by adding 0.067 g of Na_2S and 0.4 mL of HCl just before closing the conical flask for studies. Also different concentrations of H_2S (400 ppm and 700 ppm) were prepared following the same methodology mentioned before.

Table 1. Analysis of the chemical composition as well as the physical characteristics of the used formation water

Chemical constituents			Physical properties		
Ionic species	**Unit**	**Value**	**The property**	**Unit**	**Value**
Lithium	(mg/L)	0.63	Density @ 60 ˚F	g/mL	1.07468
Sodium	(mg/L)	29246	pH at 25 ˚C		7.79
Fluoride	(mg/L)	0.48	Salinity (as NaCl)	mg/L	97566.2
Chloride	(mg/L)	59131	Conductivity at 27.9 ˚C	mhos/cm	13.11×10^{-2}
Potassium	(mg/L)	445.20	Total hardness (as $CaCO_3$)	mg/L	19615.3
Magnesium	(mg/L)	1263.23	Alkalinity (as $CaCO_3$)	mg/L	116.7
Calcium	(mg/L)	5772.26	Specific gravity		1.07575
Strontium	(mg/L)	444.1	Resistivity at 27.9 ˚C	Ohm-m	0.0763
Barium	(mg/L)	135.97	Total dissolved solids	mg/L	97398.8
Bromide	(mg/L)	196.6	(T.D.S.)		
Sulfate	(mg/L)	621			
Bicarbonate	(mg/L)	142.33			

Electrochemical measurements

The previously mentioned working electrode, platinum counter electrode and reference saturated calomel electrode were used in a three-electrode cellto accomplish the electrochemical measurements. The schematic of this experimental setup is shown in Scheme 2. The scrubber system used a vessel of sodium hydroxide (usually 10 wt.% NaOH) connected to the gas outlet. This system was employed to chemically reduce the health and safety risk in dealing with H_2S in the laboratory. A potentiostat of PGZ301 Volta lab 40 (France) supplied with Voltamaster 4 software was employed to perform all electrochemical measurements. Submerging the working electrode for 1 hour in the corrosive media was carried out to get stable state open circuit potential (OCP). At 1 mV/s constant sweep rate, 25 °C, and in the range of -1100 to -300 mV, potentiodynamic polarization measurements were determined. On the other hand, the corrosion's electrochemical impedance spectroscopy (EIS) at amplitude of 10 mV, AC signals and 100 kHz to 10 mHz frequency range was assessed for various polymers and concentrations based on the plots of Nyquist and Bode. For ensuring the reproducibility, every sample was tested for 3 times.

ISSN 2349-0292
Impact Factor 3.802

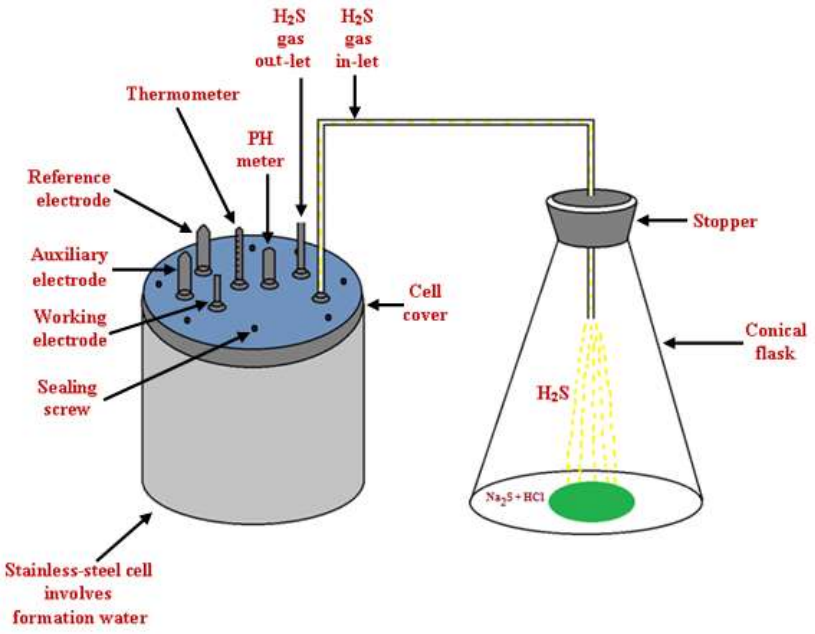

Scheme 2:Schematic of the experimental test cell.

Field emission SEM and EDX analyses

This analysis was performed to investigate the morphology of the carbon steel sample surface submerged in sour formation water in absence and presence of 100 ppm of the synthesized PSB2 inhibitor. An instrument of Quanta 250FEG field emission gun, Netherlands, captured carbon steel surface morphology images at 30 KV accelerating voltage and 14x up to 1000000 magnification power. An EDX system attached to SEM Model Quanta 250 FEG studied the chemical composition of the carbon steel surface immersed in sour well formation water as well as the inhibitor film formed on it after a definite poly Schiff base inhibitor concentration was added. Voltage signals obtained via X-ray detector that reflect the interaction between the surface of carbon steel and X-rays, were recorded and sent to the pulse processor then to an analyzer for analyzing the data.

The quantum studies

A level program of Unrestricted Hartree-Fock (UHF) with Hyperchem 8.0 based on MINDO3 semi-empirical techniquewas employed to test the inhibitors' quantum chemical calculations [19]. The E_{HOMO} and E_{LUMO} values (refer to the highest and lowest occupied molecular orbitals) can be obtained in a molecular 2-dimentional ISIS drawing, while the band gap of energy is expressed as ($\Delta E = E_{LUMO} - E_{HOMO}$). It also involves electronegativity (χ) (which express the atomic tendency to attract electrons), softness (σ), global hardness (η), affinity of electrons (A), and the potential of ionization (I); which are determined through Koopmans' theorem [20,21]. Following Koopman's theorem: χ can be determined through Eq. (1) [22]:

$$\chi \cong -1/2\ (E_{HOMO} + E_{LUMO}) \quad (1)$$

An atomic resistance for transferring a charge is termed as global hardness (η), which can be determined through Eq. (2) [23].

$$\eta \cong -1/2\ (E_{HOMO} - E_{LUMO}) \quad (2)$$

The atomic capacity for electron receiving is known as global softness (σ) [23], which can be evaluated through Eq. (3).

$$\sigma \cong -2/(E_{HOMO} - E_{LUMO}) = 1/\eta \quad (3)$$

Eq. (4) can define the affinity of electron (A), while Eq. (5) can evaluate the potential of ionization (I)

$$A \cong -E_{LUMO} \quad (4)$$

$$I \cong -E_{HOMO} \quad (5)$$

ISSN 2349-0292
Impact Factor 3.802

Eq. (6) can estimate the alternation in the number of electrons transfer.

$$\Delta N = \frac{\chi_{Fe} - \chi_{inh}}{2\eta_{Fe} - 2\eta_{inh}} \quad (6)$$

In this equation, χ_{Fe} and η_{Fe} represent carbon steel electronegativity as well as hardness (with 7 eV mol^{-1} and 0 eV mol^{-1} vales, respectively), while χ_{inh} and η_{inh} refer to inhibitor's electronegativity and hardness [24]. QSAR technique was employed to calculate the polarizability, log P as a hydrophobic factor, and the energy of hydration from the optimized geometry. Also, the polarity measurement obtained from the dipole moment (μ) can assess the distribution of electrons in a molecule.

RESULTS AND DISCUSSION

Confirmation of inhibitors' chemical composition

FTIR spectra of these prepared poly Schiff bases (PSB1, PSB2, and PSB3) were illustrated in Figure 1. For PSB1, a broad absorption peak around 3406 cm^{-1} is due to the $–NH_2$ stretching at the terminals. The result revealed the 2941cm^{-1}, 2806cm^{-1}, and 1467cm^{-1} peaks ascribed for asymmetric C-H stretch of alkane, symmetric stretch of alkane C-H bonds, and –C-H symmetric deformation of alkane, respectively. While that at 1649 cm^{-1} is due to C=N stretching in the imine group. For PSB2, the broad absorption peak around 3458 cm^{-1} is due to the$–NH_2$ stretching at the terminals. The bands at 2946 cm^{-1}, 2887 cm^{-1}, 1454 cm^{-1}, and 1641 are due to the asymmetric and symmetric C–H stretching, –C-H symmetric deformation of alkane and aliphatic stretching of C=N in the imine unit, respectively. For PSB3, the $–NH_2$ stretching at the terminals, asymmetric and symmetric C–H stretching, –C-H symmetric deformation of alkane, and aliphatic C=N stretching in the imine group are observed at 3467 cm^{-1}, 2947$cm^{-1}$and 2871cm^{-1}, 1466cm^{-1}, and 1641 cm^{-1}, respectively. In the three polymers, the bands at 1117-1276 cm^{-1} are related to C-C bond of alkane. Also, no absorption peaks were observed around 1715 cm^{-1} of C=O of aldehyde which confirm the consumption of the glutaraldehyde in the polymerization reaction [25].

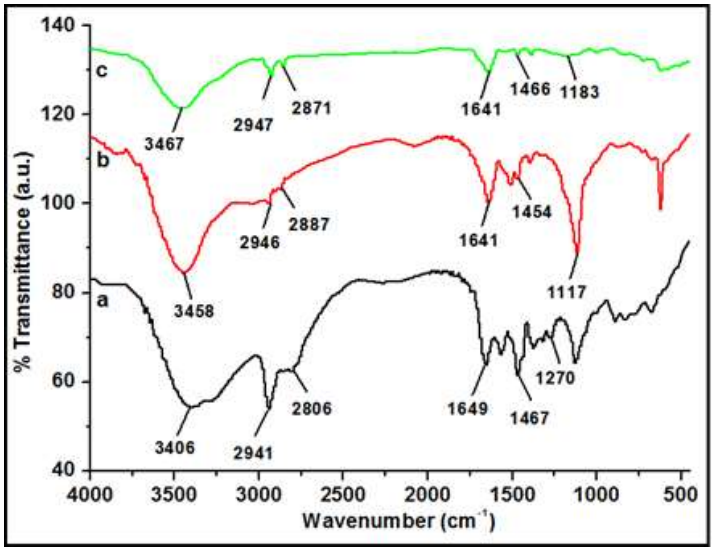

Figure 1: FTIR spectra of the prepared (a) PSB1, (b) PSB2, and (c) PSB3

^{1}HNMR spectra of the prepared Schiff base polymers (PSB1, PSB2 and PSB3) were observed at Figure 2. The ^{1}HNMR spectrum of PSB1 was illustrated in Figure 2a. The peak at 7.3 ppm is assigned to imine (-CH=N-) proton. Dufrasne et al. reported the presence of imine protons in the ^{1}HNMR analysis at 7.3-7.9 ppm, which goes in agreement with our result [26]. The shift at 3.8 ppm is due to the terminal NH_2 protons in the prepared polymer. The shifts at 1.26 ppm and 3.6 are due to CH_2 aliphatic methylene protons and -CH_2-N= protons, respectively. For PSB2 (Figure 2b), the chemical shifts observed at 7.3 ppm, 3.1ppm , 1.3 ppm and 2.6 ppm are referred to the imine (-CH=N-) protons, terminal NH_2protons, CH_2 aliphatic methylene protons and -CH_2-N= protons. For PSB3 (Figure 2c), the imine (-CH=N-) protons, terminal NH_2protons, CH_2 aliphatic methylene protons and -CH_2-N= protons were observed at 7.3 ppm, 3.7 ppm, 1.25 ppm, and 2.6 ppm, in that order. No residual aldehydes end groups were visible around 9.5 ppm [27] in all the synthesized polymers.

ISSN 2349-0292
Impact Factor 3.802

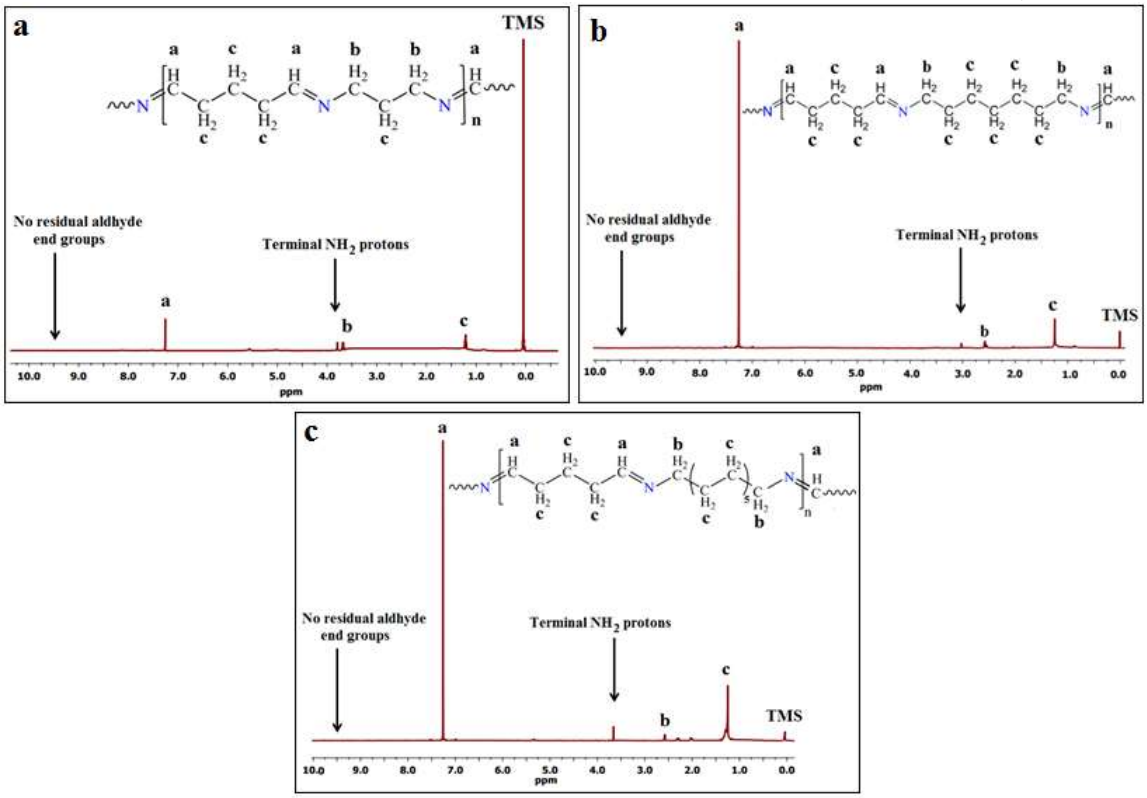

Figure 2: [1]HNMR analysis of the prepared(a) PSB1; (b) PSB2 and (c) PSB3

The Mw, Mn, and polydispersity index (PDI) of the polymeric inhibitor PSB1 were 2575 g/mol, 2489 g/mol and 1.035, respectively. For PSB2, the Mw, Mn and PDI were 4924 g/mol, 1701 g/mol and 2.895, respectively. While these measurements were 7379 g/mol, 3107 g/mol, and 2.375 for PSB3.

The thermal stability of the prepared polymers was indicated in Figure 3. TGA illustrated the thermally stable composition of PSB1 with only 10% and 50% loss in weight at 153.6 °C and 337.6 °C, respectively**.** TGA figure descended with temperature of maximum degradation (T_{max}) at 745.52 °C which might be due to the decomposition of the polymer chains. The thermal stability of PSB2 showed that T_{-10}, T_{-50} and T_{max} were observed at 212.3 °C, 324.5 °C and 783.4 °C which indicated the highest thermal stability among the prepared polymers. Also, the thermal stability of PSB3 showed that T_{-10}, T_{-50} and T_{max} were observed at 251.7 °C, 410.7 °C and 698 °C, respectively.

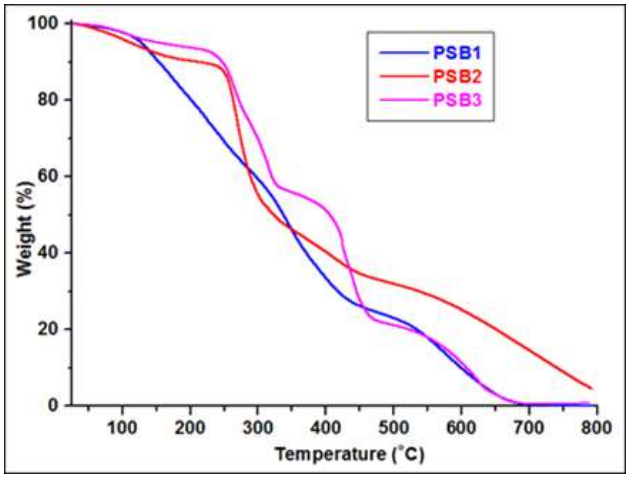

Figure 3: TGA analysis of the prepared PSB1, PSB2, and PSB3 polymeric inhibitors

ISSN 2349-0292
Impact Factor 3.802

Mechanism of corrosion inhibition

Corrosion inhibition of carbon steel in sour formation water by using our prepared Schiff base polymers can be explained on the basis of molecular adsorption as illustrated in Scheme 3. In sour solution, polymers exist as protonated species. The nitrogen atoms present in polymers can be easily protonated in acidic solution and convert into quaternary compounds. These protonated species adsorbed on the cathodic sites of the carbon steel and decrease the evolution of hydrogen. The adsorption on anodic site occurs through pi-electrons of imine group and lone pair of electrons of nitrogen atoms which decrease the anodic dissolution of carbon steel [28].

The high performances of polymers are attributed to the presence of pi-electrons, nitrogen atom and the planarity of compounds. Thus polymers can adsorb on the carbon steel surface by following ways:

(a) Electrostatic interaction between the charged molecules and charged metal;

(b) Interaction of π-electrons with the metal;

(c) Interaction of unshared pair of electrons in the molecule with the metal; and (d) The combination of the all the effects [29, 30].

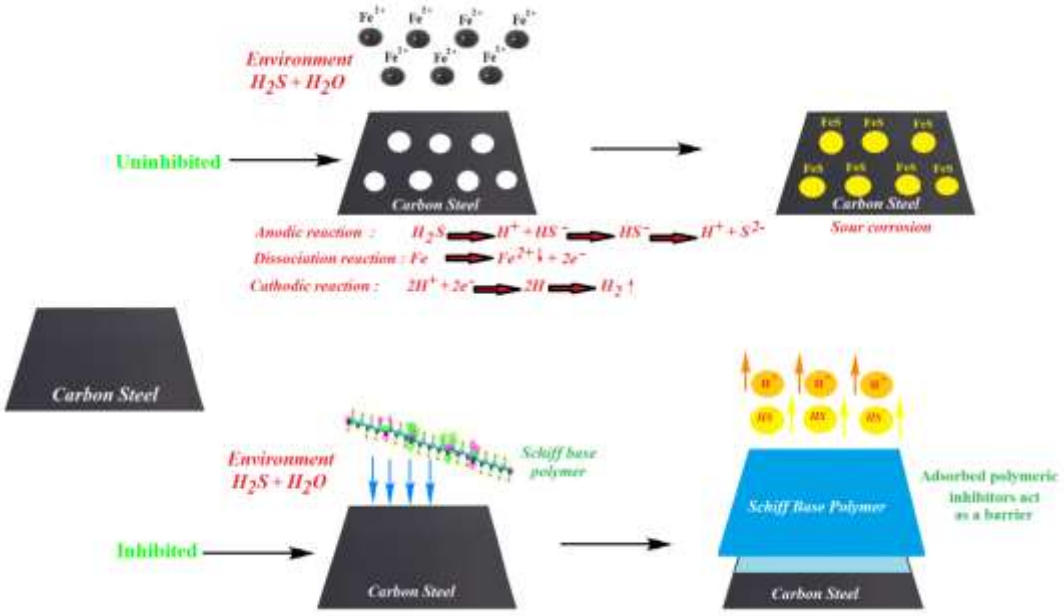

Scheme 3: Mechanism of corrosion inhibition of the prepared Schiff base polymers for carbon steel samples in sour formation water

Open circuit potential (OCP)

It was determined for carbon steel electrode immersed inside the sour well formation water (including various H_2S concentrations) as a function of the time of submersion in the media without and with various concentrations of PSB inhibitors. More negative potential was recorded for the carbon steel electrode submerged inside the sour media and supplied with 100 ppm of H_2S (blank curve) as illustrated in Figure 4 for PSB2 inhibitor as a representative sample, giving rise to short step of forming $Fe(OH)_3$ intermediate. This is caused by breaking down of the surface's air formed oxide layer following Eq. (7):

$$Fe_2O_3 + 3H_2O \rightarrow 2Fe(OH)_3 \quad (7)$$

New oxide layer was grown in the media with directing toward more noble direction to get a steady state potential. A positive shift in the OCP was produce by adding inhibitor molecules to the aggressive medium, because of the anodic reaction retardation caused by metal dissolution processing [31].

ISSN 2349-0292
Impact Factor 3.802

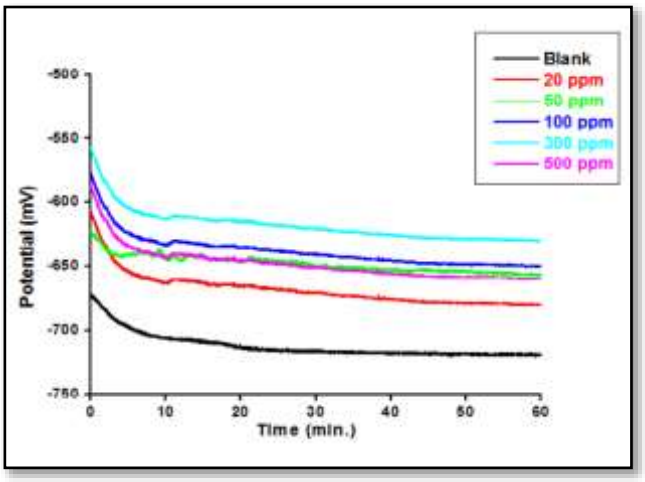

Figure 4: A potential-time plot for the carbon steel surface submerged in the oils wells media containing 100 ppm of H_2S without and with various PSB2 inhibitor concentrations

Determinations of the Potentiodynamic polarization

Figure 5 illustrated the carbon steel sample's cathodic and anodic polarization diagrams after submerged inside sour formation water that contain H_2S (100 ppm) with different PSB1, PSB2, and PSB3 concentrations. Also Figure 6 shows carbon steel sample's diagram of potentiodynamic polarization after submerged in the sour media containing 400 ppm and 700 ppm of H_2S without and with100 ppm concentration of PSB1, PSB2 and PSB3 inhibitors.

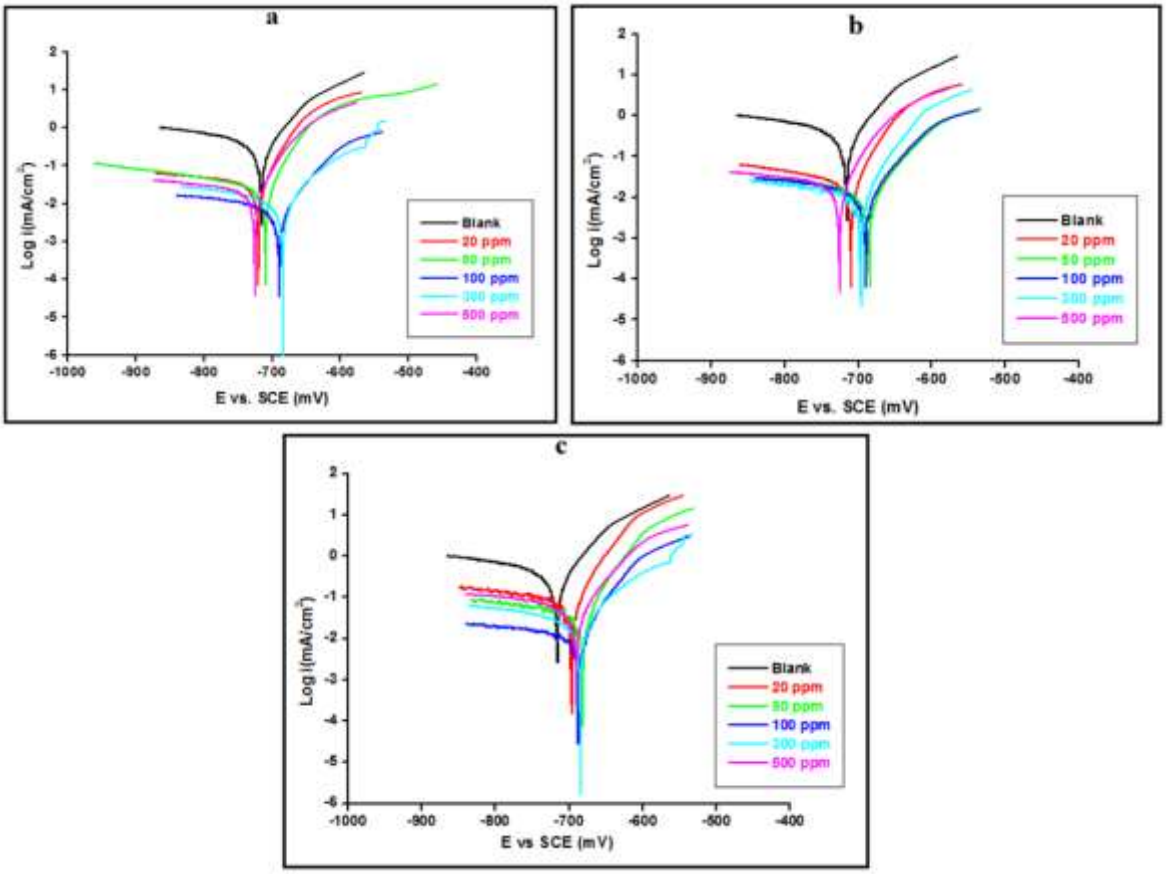

Figure 5: A plot for Potentiodynamic polarization of carbon steel surface submerged in oils wells media that was supplied with 100 ppm of H_2S without and with different concentrations of (a) PSB1; (b) PSB2; and (c) PSB3 inhibitors at 25 ˚C

ISSN 2349-0292
Impact Factor 3.802

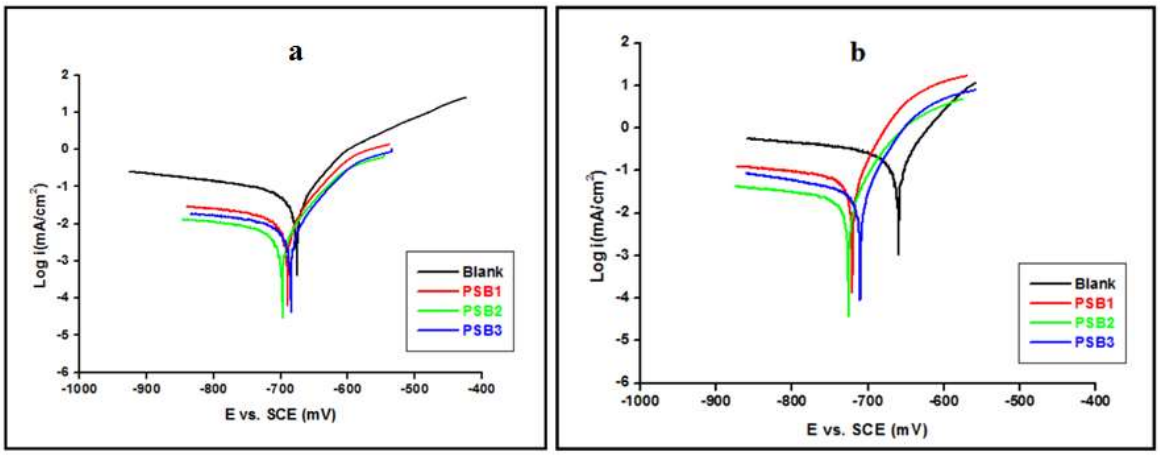

Figure 6: A plot for potentiodynamic polarization of carbon steel surface submerged in the oils wells formation media including (a) 400 ppm and (b) 700 ppm of H_2S without and with 100 ppm of each (PSB1, PSB2, and PSB3) inhibitor at 25 °C

The potential of corrosion ($E_{corr.}$), current density of corrosion ($i_{corr.}$), resistance of polarization (R_p) as well as the anodic and cathodic slopes of Tafel (β_a and β_c) were calculated and are listed in Tables (2 and 3). These data reflected that i_{corr} decreases with raising the concentration of inhibitor up to 300 ppm for PSB2 and up to 100 ppm for PSB1 and PSB3 as compared with the blank solution. Moreover, further increase in the concentration causes a slight reduction in the corrosion current density. With increasing PSB2 concentration from 20 to 300 ppm and to 100 ppm for PSB1 and PSB3, the corrosion inhibition increased gradually which is caused by well distribution of the inhibitor as a thin defensive film on the whole surface of carbon steel. This thin film can cover the entire surface without any voids or bits with enhanced bonding strength between the anticorrosive layer and metal surface. On the other hand, higher concentration of poly Schiff base inhibitors results in agglomeration which reduces the metal–inhibitor film bond strength. Inhibitors' molecules are adsorbed as a thin layer over carbon steel surface through their flat orientation when the concentration is below the optimum value. As a result, the inhibitor's concentration enhanced the layered film on the surface [32]. After reaching the concentration of optimum (maximum coverage of the surface), any increase in the concentration of inhibitor may increase the intermolecular repulsion forces between the molecules of inhibitor [33] which reduced the inhibition effect and enable corrosive media to attack the surface. Eqs. (8 and 9) can determine the surface coverage of carbon steel by the inhibitor as well as the inhibition efficacy percentage which are expressed as θ and η_p%, respectively [34]. The densities of the current corrosion without and with inhibitor were abbreviated as $i°$ and i, respectively:

$$\theta = \frac{i° - i}{i°} \quad (8)$$

$$\eta_p\% = \theta \times 100 \quad (9)$$

Anodic and cathodic Tafel slopes are slightly affected by enhancing or reducing the inhibitor concentration as the inhibitor has an effect on both anodic and cathodic interactions. Consequently, these prepared inhibitors were categorized as an inhibitor of mixed-type [35]. The formed adsorption film on the carbon steel's cathodic and anodic reactive sites can extremely inhibit both cathodic and anodic reactions [36]. The molecules of inhibitor influence the carbon steel's rate of corrosion without any alternation in the mechanism of metal dissolution as indicated from the trivial variation in the Tafel plots of anodic and cathodic directions [37]. From results in Tables (2 and 3), it is indicated that η_p% of PSB2 inhibitor is greater than that of PSB1 and PSB3 polymers. Such inhibitory action of Schiff base polymers with different carbon chain length follows Traube's rule in which the inhibition efficiency increases with increasing chain length of polymers up to 11 or 12 -CH_2 units. More methylene groups in the chain length can reduce or remain the polymeric inhibition tendency [38].

ISSN 2349-0292
Impact Factor 3.802

Table 2. Electrochemical factors gotten from the polarization plots of PSB1, PSB2 and PSB3 Inhibitors at 25 °C in presence 100 ppm of H_2S

Inhibitor	Conc. (ppm)	E_{corr} (mV vs. SCE)	i_{corr} (mA cm^{-2})	$R_p\Omega.cm^2$	β_a (mV dec^{-1})	β_c (mV dec^{-1})	η_p%
Blank	0	-716.2	0.0971	669	89.4	-332.0	-
PSB1	20	-720.2	0.0341	805.21	42.9	-554.1	64.88
	50	-709.7	0.0318	992.83	44.3	-466.9	68.14
	100	-689.2	0.0168	1080	51.3	-367.4	82.69
	300	-684.1	0.0193	1010	85.0	-400.6	80.12
	500	-725.3	0.0210	662.65	49.7	-495.8	78.37
PSB2	20	-709.7	0.0237	833	44.3	-349.3	75.60
	50	-684.1	0.0135	1058	85.0	-400.6	86.10
	100	-689.2	0.0098	1069	51.3	-367.4	89. 80
	300	-696.8	0.0096	1093	41.8	-340.4	90.21
	500	-725.3	0.0155	999	49.7	-494.5	84.03
PSB3	20	-696.3	0.0524	715.17	41.8	-340.	46.44
	50	-683.5	0.039	769	44.3	-466.9	59.83
	100	-687.5	0.0192	1065	155.6	-496.0	80.22
	300	-685	0.0225	945.34	85.0	-400.6	72.19
	500	-690.5	0.042	712.83	51.3	-367.4	56.74

Table 3. Electrochemical factors determined through EIS and polarization curves of 100 ppm of PSB1, PSB2 and PSB3 Inhibitors at 25 °C in presence 400 ppm and 700 ppm of H_2S

Inhibitor	Conc. (ppm)	R_s ($\Omega.cm^2$)	R_{ct} ($\Omega.cm^2$)	C_{dl} (μFcm^2)	η_z%	E_{corr} (mV vs. SCE)	i_{corr} (mA cm^2)	R_p ohm.cm^2	β_a (mV dec^{-1})	β_c (mV dec^{-1})	η_p%
Blank	400 ppm	21.51	398.1	284.5	-	-674.2	0.12	535.64	67.4	-332.0	-
	700 ppm	5.12	112.3	158.6	-	-660.7	0.1673	138.69	60.5	-591.6	-
PSB1	400 ppm	27.17	1189	133.7	66.51	-691.1	0.0343	697.19	43.4	-397.8	71.6
	700 ppm	4.43	251.0	95.4	55.25	-720.4	0.0683	152.60	42.9	-554.5	59.28
PSB2	400 ppm	33.47	2140	112.3	81.39	-697.1	0.0213	1036	49	-327.8	82.5
	700 ppm	3.6	516.9	73.4	78.28	-724.6	0.0345	402.33	49.7	-494.5	79.59
PSB3	400 ppm	39.02	2117	115.2	81.19	-684.9	0.0242	927	44.8	-257.1	80.00
	700 ppm	3.2	353.7	80.3	68.24	-710.6	0.0512	246.41	44.3	-348.8	69.7

EIS measurements

Without and with addition of various inhibitor concentrations at 25 °C, carbon steel's impedance in the sour formation water supplied with 100 ppm of H_2S were measured as shown in Figure 7. Moreover, thecarbon steel corrosion in the sour formation water containing 400 ppm and 700 ppm of H_2S (without and with adding 100 ppm of PSB1, PSB2, and PSB3 inhibitors) was also investigated by EIS technique (Figure 8). The carbon impedance was considerably affected by inhibitor molecule addition as reflected from Nyquist plots. The increases in the resistance of chargetransfer (R_{ct}) as well as reduction in the capacitance of double layer (C_{dl}) are recorded for the enhanced inhibitor concentrations. This was affected by enhancing the electrical double layer thickness and reducing the local dielectric constant, which reflected the adsorption mechanism of inhibitor molecules at carbon/inhibitor interface [39].

ISSN 2349-0292
Impact Factor 3.802

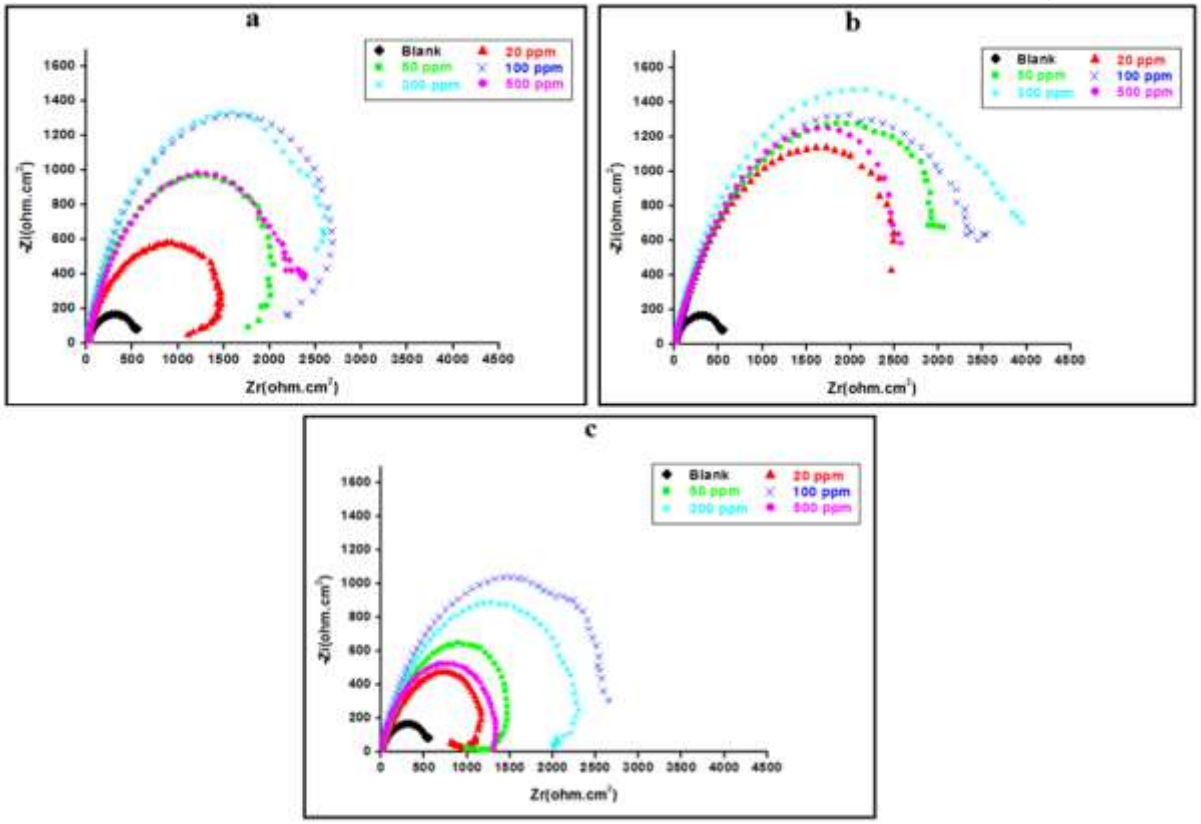

Figure 7: Nyquist curve for the carbon steel surface immersed in oils wells formation media containing 100 ppm of H_2S without and with different concentrations of (a) PSB1; (b) PSB2, (c) PSB3 inhibitors at 25°C

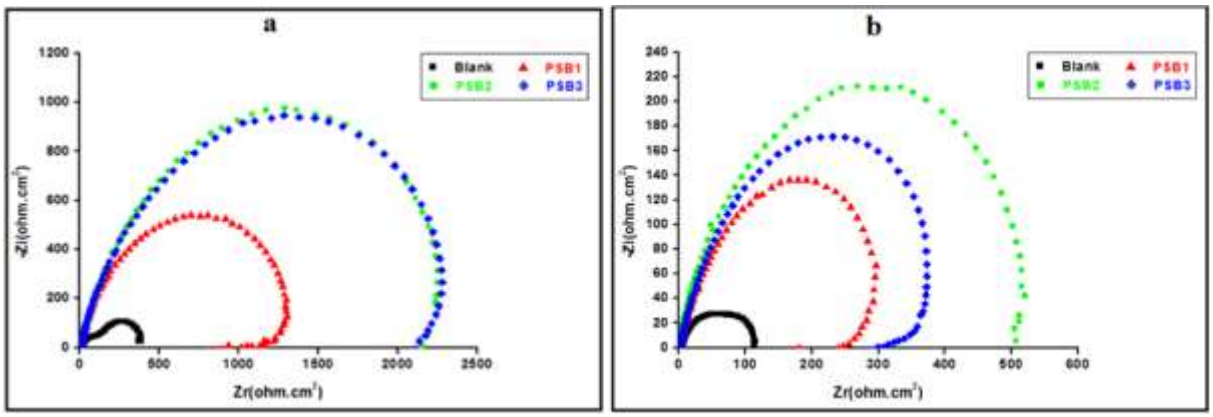

Figure 8: Nyquist curve of carbon steel surface in the used formation media containing (a)400 ppm (b) 700 ppm of H_2S without and with 100 ppm of (PSB1, PSB2, and PSB3) inhibitors at 25 °C

In addition of synthesized inhibitors, lower C_{dl} values were gotten for the prepared polymer inhibitors because the inhibitor was adsorbed on the carbon steel surface. EIS evaluations agree completely with those achieved from the potentiodynamic polarization. Tables (3 and 4) indicate the calculated R_{ct}, C_{dl}, and percentage inhibition efficiency (η_z%). The η_z% of metal corrosion was obtained through R_{ct}as mentioned in Eq. (10) [40]:

$$\eta_z\% = \frac{R_{ct} - R^{\circ}_{ct}}{R_{ct}} \times 100 \qquad (10)$$

Where R_{ct} and $R°_{ct}$ represent electrode resistance of charge transfer in the presence and absence of polymeric inhibitor.

ISSN 2349-0292
Impact Factor 3.802

Table 4. Electrochemical factors determined from EIS of the PSB1, PSB2 and PSB3 Inhibitors at 25 °C in the presence of 100 ppm of H_2S

Inhibitor	Conc. (ppm)	R_s (Ω.cm²)	R_{ct} (Ω.cm²)	C_{dl} (µF cm²)	η_z %
Blank	0	4.45	597.8	473.8	-
	20	8.84	1464	217.3	59.17
	50	4.09	2097	140.3	71.49
PSB1	100	1.72	2697	120.1	77.83
	300	3.92	2645	121.2	77.39
	500	3.70	2528	125.2	76.35
	20	9.09	2843	283.7	78.97
	50	2.41	3498	107.6	82.91
PSB2	100	3.44	3827	97.5	84.37
	300	1.98	4329	85.8	86.19
	500	4.82	3064	100.3	80.48
	20	3.90	1051	211.8	43.12
	50	7.50	1337	208.0	55.28
PSB3	100	6.60	2982	116.9	79.95
	300	6.15	2199	144.7	72.81
	500	3.38	1206	205.5	50.43

Figure 9 indicated the equivalent circuit (EC) determined through Zsimpwin software for EIS analysis; where the resistance of solution (R_s), resistance and capacitance accompanied with the passive film of inhibitor (R_f and C_f, respectively) were evaluated [41]. Also, the electrical double layer capacitance (C_{dl}) and charge transfer resistance (R_{ct}) at the interface of electrolyte/metal media were assessed [42]. EIS measurements reflected a higher η_z % for PSB2 than PSB1 and PSB3 materials, which agree with the previously measured potentiodynamic polarization.

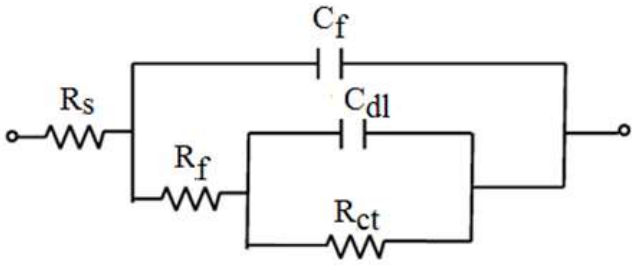

Figure 9:The electrochemical equivalent circuits for measuring the corrosion inhibition by the prepared poly Schiff bases on the metallic surface

Corrosion attack morphology

The carbon steel surface morphology after 24 hours of submersion in uninhibited (blank) and inhibited formation water at two different concentrations of H_2S (100 ppm and 700 ppm) was studied through FESEM images as indicated in Figure 10. Figure 10 (a) illustrated the FESEM capture of the carbon steel surface after polishing. On the carbon steel surface, the sizes of corrosion cavities were increased as H_2S concentration was increased from 100 ppm to 700 ppm (Figure 10 (b and c)). On contrarily, a less attack is observed for 100 ppm of PSB2 inhibitor immersed in the formation water containing 100 ppm of H_2S, where the surface was nearly unchanged (Figure 10 (d)). Also in the presence of 100 ppm of PSB2 in formation water containing 700 ppm of H_2S, the number of corrosion pits is decreased and became shallow as shown in Figure 10 (e). These images reflected the high corrosion inhibition and metallic surface protection caused by using PSB2 inhibitor.

ISSN 2349-0292
Impact Factor 3.802

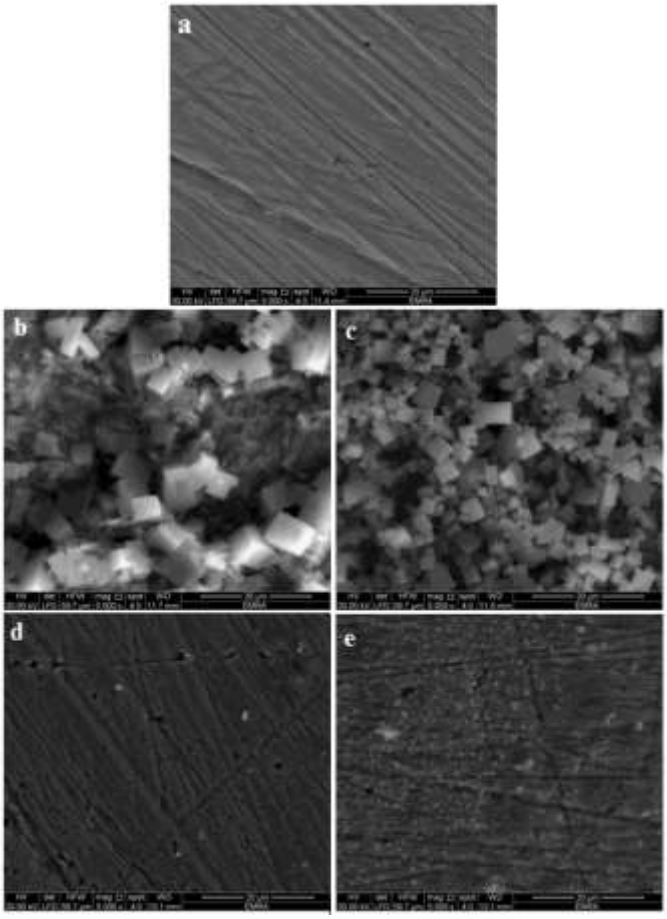

Figure 10: FESEM captures of metal surface; where (a) sample after polishing, (b) after submersion inside sour formation water including 100 ppm of H_2S, (c) after submersion inside sour formation water including 700 ppm of H_2S, (d) after submersion inside sour formation water including 100 ppm of H_2S with 100 ppm inhibitor of PSB2 and (e) after submersion inside sour formation water including 700 ppm of H_2S with 100 ppm of PSB2 inhibitor

EDX analysis

EDX analyze the elemental composition of the polymeric passive layer formed over the carbon steel surface. Figure 11 (a) reflected such polished carbon steel elemental analysis and exhibited well surface features. After submersion in sour media containing different hydrogen sulfide concentrations (100 ppm and 700 ppm) for 24 hours in the absence of poly Schiff base inhibitor, EDX analysis of the carbon steel reflected a strong damage caused by an outer corrosion (Figure11 (b and c)); where the signal of oxygen is reflected the exposure of the metal surface to the sour formation solution without inhibitor. Sulphur was shown in the EDX analyses of the blank samples after immersion in sour H_2S solution, which reflected the deposition of the metal surface with sulphide after immersion. By adding 100 ppm of PSB2 polymer, the peak of iron was reduced and the surface morphology was developed as a result of forming adhesive passive inhibitor layer over the carbon steel surface (Figure 11 (d and e)). This passive film was reflected through nitrogen presence in the EDX spectra. The presence of sulphur peak indicated that a passive film of poly sulphide was formed on the carbon steel surface to provide extra corrosion inhibition [43,44]. Strongly adhered inhibitor layer was filmed over the surface of carbon steel and afforded a high corrosion inhibition [45].

ISSN 2349-0292
Impact Factor 3.802

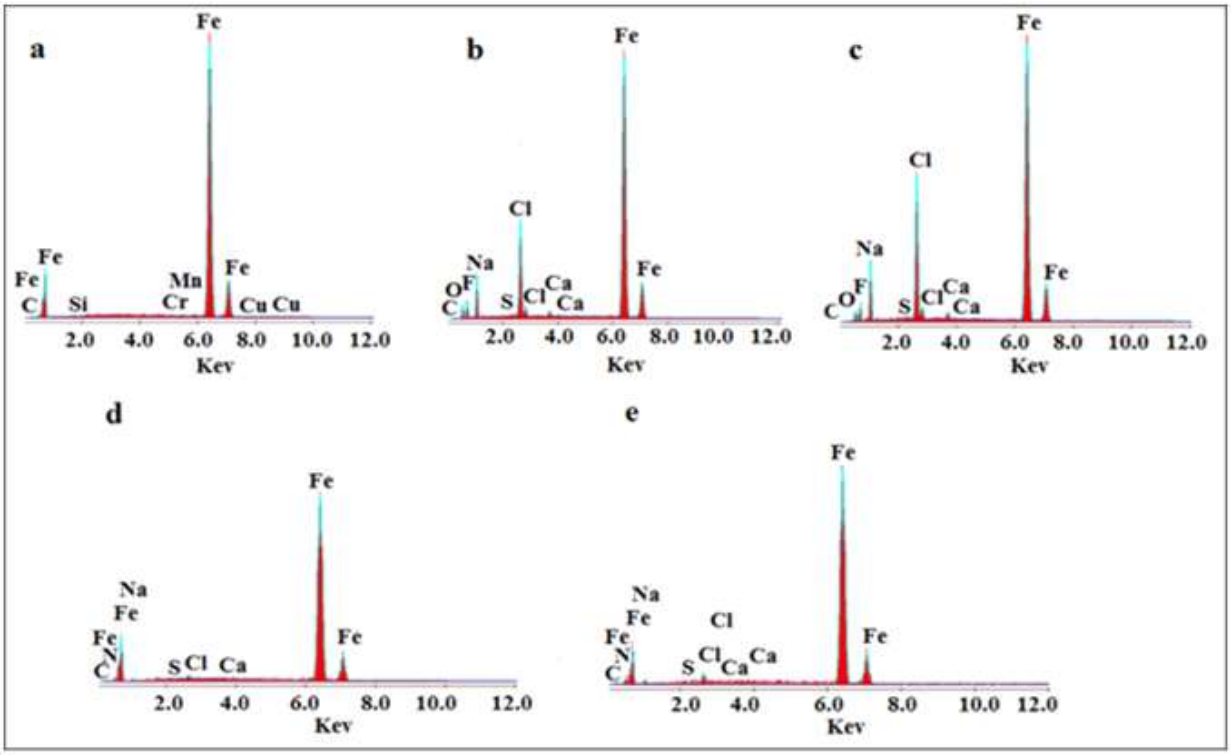

Figure 11: EDX of the metal specimens: (a) carbon steel after polishing, (b and c) samples after immersed in oil well formation water containing (100 ppm and 700 ppm) of H_2S, respectively and (d and e) samples after submersion in the sour formation water including (100 ppm and 700 ppm) of Hydrogen sulfide, respectively, with 100 ppm of PSB2

Quantum chemical calculations

Electronic and spatial molecular structures have a relationship with the corrosion inhibition efficiency; this relationship can be studied through a quantum chemical method. Tables (5 and 6) involved the measured parameters through the Quantum Chemical method, while Figure 12 showed the adjusted geometry of the inhibitors and their frontier molecule orbital density distribution.

Parallel adsorption

This factor has a correlation with the corrosion inhibition on the surface of carbon steel. It can be improved through existence of more adsorption active centers on the metal. Such active center is the present of nitrogen atoms in imine groups in their chemical structures. Inhibitor's planar geometry can afford molecular adsorption when molecular plane is parallel to the metallic surface. This enables donation and back donation between carbon steel and the inhibitor molecule. Figure 12 represented the polymeric inhibitor's planar stricture which displayed an extremely large inhibitor-metal contact area.

ISSN 2349-0292
Impact Factor 3.802

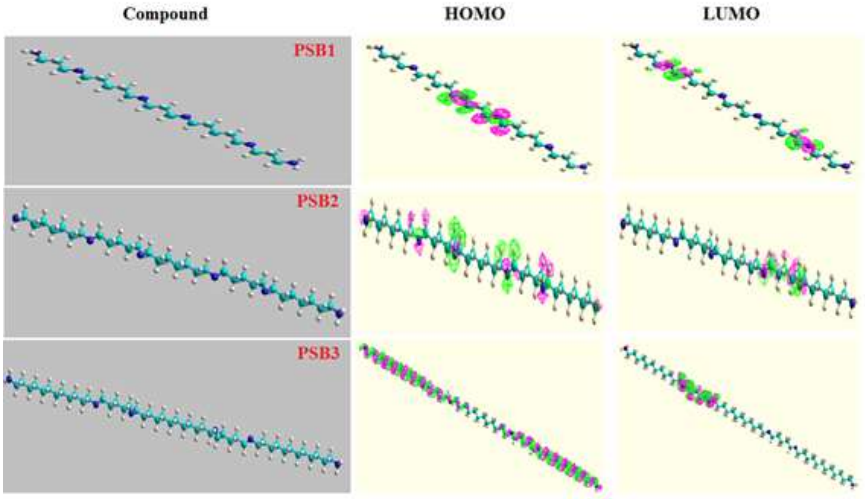

Figure 12: Optimized geometry of inhibitors and their density distribution of the frontier molecule orbitals.

Molecular orbital energies

These energies represent the most prevalent quantum chemical factors and include the highest and lowest occupied molecular orbital energies of the inhibitor (E_{HOMO} and E_{LUMO}, respectively) as mentioned in Figure 12. These orbital are termed frontier orbitals determines the interaction route between species. Higher ability to accept electrons is connected with lowering E_{LUMO}, while higher E_{HOMO} prefers electron donation to an acceptor molecule (with lower energy). The band gap between the two energies (E_{LUMO}– E_{HOMO}) of a polymeric material can be expressed as ΔE. It is a measure of the polymer softness and hardness; where large ΔE reflects hard molecular structure and vice versa [46]. Higher ΔE values reflect a harder structure than lower ΔE structures which exhibit softer moieties. The results also showed a reduction in ΔE following the order PSB3<PSB2 <PSB1 with values of 10.21, 10.57 and 10.72, respectively. PSB2 has an intermediate value between PSB1 and PSB3.

Dipole moment (μ)

This factor reflects the inhibitor molecule hydrophobicity [47]. It was reported that the corrosion inhibition has no substantial relationship to the dipole moment evaluations. Also, the correlation between the corrosion efficiency and dipole moment suffer from insufficient literature agreement [48].

Interestingly, in the current work, there is an irregularity that appeared in the case of correlation of the dipole moment with the inhibition efficiency as illustrated in Table 5. The PSB2 inhibitor which exhibits high inhibition efficiency has an intermediate dipole value which is higher than PSB3 and lower than PSB1.

Table 5. Quantum chemical factors determined for the prepared polymeric inhibitors

Inhibitor	E_{HOMO}(eV)	E_{LUMO} (eV)	ΔE (eV)	μ (debye)	Log P	ΔN
PSB1	-9.21	1.51	10.72	5.54	-1.54	0.293
PSB2	-8.83	1.74	10.57	3.27	3.38	0.326
PSB3	-8.66	1.55	10.21	2.10	9.33	0.337

Lipophilicity coefficient (Log P)

It is affected by the polymer's hydrophobic nature. Inhibitors with low Log P, prefer water environment, and can undergo adsorption over metal surface that accept electrons in its outer orbital. The results indicated the increasing in the hydrophobicity and corrosion inhibition by using the prepared polymers in the order PSB1 < PSB2 < PSB3 which affected by the existence of imine bonds. PSB2 has an intermediate value between PSB1 and PSB3, but the practical results reflected its higher efficiency as previously discussed.

The transferred electrons number (ΔN)

This value expresses the inhibition efficiency through electron donation from the polymeric inhibitor toward metallic surface. Following Lukovits's hypothesis [49], if ΔN < 3.6, electron donation from such inhibitor to the metallic surface is increased, that resulted in increasing the corrosion inhibition. Table 5 reported the ΔN values which refer to the electronic charges numbers exchanged between the adsorbed inhibitor and the metallic

ISSN 2349-0292
Impact Factor 3.802

surface. Herein, inhibitor PSB2 is experimentally expected to have higher corrosion inhibition efficiency. ΔN measurements of PSB2 and PSB3 are very close and are higher than PSB1 (Table 5) which confirmed an enhancement in the efficacy of inhibition with enhancing ΔN value.

Ionization potential (I)

It is in a direct correlation with E_{HOMO}. Ionization potential determinations of PSB2 and PSB1 are very close like their values in E_{HOMO} and are higher than PSB3. So PSB2 has a high ionization potential value that confirms its higher inhibition efficiency toward corrosion than other inhibitors.

Electron affinity (A)

The negative values of *A* reflect the capability of inhibitor molecule to be electrophilic. Increasing the inhibitor ability for accepting electrons form the metal surface, yields increased *A* value as well as high efficiency of inhibition to protect the metal surface. PSB2 was reported to be the best corrosion inhibitor among the three prepared poly Schiff bases because of the highest *A* value as recorded in Table 6.

Table 6. Additional calculated quantum chemical factors for the prepared polymeric inhibitors

Inhibitor	Ionization Potential, *I* (eV)	Electron Affinity, *A* (eV)	Electronegativity of the whole inhibitor ($eVmol^{-1}$)	Electronegativity of the active center ($eVmol^{-1}$)	Global Hardness ($eVmol^{-1}$)	Softness, $\sigma = 1/\eta_{inh}$ (eV^{-1})
PSB1	9.21	-1.51	3.85	-1.02	5.36	0.186
PSB2	8.83	-1.74	3.545	-1.58	5.285	0.189
PSB3	8.66	-1.55	3.555	-1.23	5.105	0.195

Electronegativity (χ)

It represents the molecule's capability to attract electrons and gain electronic negative charge. Thus, the electronegativity and hardness can predict the chemical behavior. Through interaction between the poly Schiff base inhibitor (low electronegativity) and carbon steel (high electronegativity), the electrons transfer from the donor inhibitor molecule toward the acceptor carbon steel till equal chemical potentials are achieved [50]. This produce larger inhibitor's electronic chemical potential than that of carbon steel (-7 $eVmol^{-1}$), which allow the electron transfer from the polymeric inhibitor toward the metal.

The lowest electronegativity and the highest corrosion protection were reported for PSB2 inhibitor (Table 6). All the electronegativity values of the inhibitors were lower than the values for steel (7 eV mol^{-1}), while greater values of electronic chemical potential for the inhibitor than those for carbon steel(which has -7 $eVmol^{-1}$) was reported. Thus the electrons transfer from the highest chemical potential (inhibitor) to the lowest chemical potential (the iron).

Active center Electronegativity

More corrosion protection and better adsorbed inhibitor film of the metal surface was produced via donor-acceptor interaction by more negatively charged heteroatom; which provide more inhibitor's atomic partial charges and facilities the electron donation. Thus, more electrostatic attraction between carbon steel surface and the inhibitor was obtained. The nitrogen atoms' electronegativity present in the polymeric inhibitors can be estimated. Increasing the nitrogen electronegativity and, as a result, the inhibition efficiency is in the order of PSB2 > PSB3 > PSB1 with values of -1.58 > -1.23 > -1.02 $eVmol^{-1}$ as shown in Table 6.

Global hardness (η)

It expresses the molecules reactivity and nearly equals ΔE/2. A high **η** value reflects the polymer's high stability and low reactivity. The global hardness values of PSB2 and PSB3 are very close and lower than PSB1 values as shown in Table 6, which indicates the high effectiveness of PSB2 and PSB3 polymers to be used as corrosion inhibitors.

Softness (σ)

A softer polymer shows high reactivity than a harder one because of the reduced ΔE energy [51]. Table 6 showed that PSB2 and PSB3 have a very close softness evaluations and are higher than PSB1 value that reflected their adsorption enhancement on the surface carbon steel with corrosion inhibition improvement.

CONCLUSIONS

A facile polycondensation method was used to prepare three poly Schiff bases which were characterized through FTIR, ^{1}HNMR, GPC and TGA. The prepared Schiff base polymers cause high corrosion inhibition for carbon steel samples immersed inside oils wells formation water with various H_2S concentrations. With increasing the inhibitor concentration (up to 300 ppm for PSB2 and 100 ppm for PSB1 and PSB3), the efficiency of corrosion inhibition was improved. The prepared poly Schiff bases represented mixed type inhibitors as indicated from the polarization curves. The C_{dl} reduction with increasing the concentrations of poly Schiff bases until optimum concentration for each one indicated that the corrosion inhibition goes through two mechanisms: (1) geometric blocking mechanism which reduce the existence reaction area, and (ii) inhibition mechanism through adjusting the energy of activation for anodic and cathodic interactions on the carbon steel surface. PSBs cause high corrosion inhibition by forming a strongly adhered protective film to cover the carbon steel. This film protects carbon steel surface from the corrosive media through inhibition mechanism which increased in the following order PSB1< PSB3 < PSB2 according to Traube's rule in which the inhibition efficiency enhanced with enhancing the polymeric chain length up to 11 or 12 -CH_2 units, while with increasing the chain length (more methylene units) the inhibition efficiency was reduced or remains unchanged (based on the polymeric type). The formation of excellent protective film of the best inhibitor PSB2 over the carbon steel was elucidated via FESEM and EDX analyses. The correlation between the inhibition efficiencies of the prepared PSBs toward carbon steel corrosion in sour petroleum conditions and their quantum chemical parameters were assessed through the quantum chemical calculations.

REFERENCES

[1] M. V. Azghandi, A. Davoodi, G. A. Farzi, A. Kosar, Water-base acrylic terpolymer as a corrosion inhibitor for SAE1018 in simulated sour petroleum solution in stagnant and hydrodynamic conditions, Corros. Sci. 64 (2012) 44–54.

[2] (a) S. Sun, W. Chen, S. Yi, S. Cao, Study of the corrosion protection behavior of neutral water-based rust remover on carbon steel, Coll. Surf. A: Physicochem. Engin. Aspects 558 (2018) 130-137; (b) Y. Liu, N. Liu, Y. Jing, X. Jiang, L. Yu, X. Yan, Surface design of durable and recyclable superhydrophobic materials for oil/water separation, Coll. Surf. A: Physicochem. Engin. Aspects 567 (2019) 128-138.

[3] A. M. Al-Sabagh, N. M. Nasser, O. E. El-Azabawy, A. E. El- Tabey, Corrosion inhibition behavior of new synthesized nonionic surfactants based on amino acid on carbon steel in acid media, J. Mol. Liq. 219 (2016) 1078–1088.

[4] P.R. Roberge, V. S. Sastri, Laboratory and field evaluation of organic corrosion inhibitors in sour media, Corros. Sci. 35 (1993) 1503–1513.

[5] D. V. Gonçalves, M. A. G. Paiva, J. C. A. Oliveira, M. Bastos-Neto, S. M. P. Lucena, Prediction of the monocomponent adsorption of H2S and mixtures with CO2 and CH4 on activated carbons, Coll. Surf. A: Physicochem. Engin. Aspects 559 (2018) 342-350.

[6] M. Xu, Q. Zhang, Z. Wang, J. Liu, Z. Li, Cross impact of CO2 phase and impurities on the corrosion behavior for stainless steel and carbon steel in water-containing dense CO2 environments, Int. J. Greenhouse Gas Control. 71 (2018) 194-211.

[7] A. H. Jalili, M. Shokouhi, F. Samani, M. Hosseini-Jenab, Measuring the solubility of CO2 and H2S in sulfolane and the density and viscosity of saturated liquid binary mixtures of (sulfolane+CO2) and (sulfolane+H2S), J. Chem. Thermodynam. 85 (2015) 13-25.

[8] P. Jha, U. Mondal, D. Gogoi, G. Singh, S. Sen, Novelties of selective triphasic synthesis of bis-(p-chlorobenzyl) sulfide using hydrogen sulfide and reusable phase transfer catalyst, J. Mol. Catal. A: Chem. 418-419 (2016) 30-40.

[9] S. Paul, A. Pattanayak, S. K. Guchhait, Corrosion behavior of carbon steel in synthetically produce oil field seawater, Inter. J. Metals 2014 (2014) 1-11.

[10] M. Diaz-Cruz, M. A. Dominguez-Aguilar, A. Cervantes-Tobon, B. Castro-Dominguez, F. Jimenez-Cruz, M. T. Fuentes-Romero, Corrosion inhibition of pipeline steel X-70 in sour brine by an imidazoline derivative under flow assisted conditions, Inter. J. Electrochem. Sci. 12 (2017) 7481-7501.

[11] S. J. Kim, K. Y. Kim, A Review of corrosion and hydrogen diffusion behaviors of high strength pipe steel in sour environment, J. Weld. J. 32 (2014) 13-20.

[12] X. Xing, J. Wang, Q. Li, W. Hu, J. Yuan, A novel acid-responsive HNTs-based corrosion inhibitor for protection of carbon steel, Coll. Surf. A: Physicochem. Engin. Aspects 553 (2018) 295-304.

[13] M. R. Vinutha, T. V. Venkatesha, Review on mechanistic action of inhibitors on steel corrosion inacidic media Portugaliae Electrochim.Acta, 34 (2016) 157-184.
[14] V. Branzoi, F. Branzoi, M. Baibarac, The inhibition of the corrosion of Armco ironin HCl solutions in the presence of surfactants of the type of N-alkyl quaternaryammonium salts, Mater. Chem. Phys. 65 (2000) 288–297.
[15] F. Bentiss, M. Lebrini, M. Lagrenée, M. Traisnel, A. Elfarouk, H. Vezin, The influence of some new 2,5-disubstituted 1,3,4-thiadiazoles on the corrosion behaviour of mild steel in 1M HCl solution: AC impedance study and theoretical approach, Electrochim. Acta 52 (2007) 6865–6872.
[16] S. A. Ali, M. T. Saeed, Synthesis and corrosion inhibition study of some 1,6- hexanediamine-based N,N-diallyl quaternary ammonium salts and their polymers, Polymer 42 (2001) 2785–2794.
[17] L. H. Madkour, Elroby SK, Correlation between corrosion inhibitive effect and quantum molecular structure of Schiff bases for iron in acidic and alkaline media, Stand. Sci. Res. Essays. 2 (2014) 680-704.
[18] S. A. Umoren, Polymers as corrosion inhibitors for metals in different media, Open Corros. J. 2 (2009) 175–188.
[19] K. F. Khaled, The inhibition of benzimidazole derivatives on corrosion of iron in 1 M HCl solutions, Electrochim. Acta, 48 (2003) 2493-2503.
[20] A. M. Al-Sabagh, N. M. Nasser, E. A. Khamis, T. Mahmoud, Synthesis of non-ionic surfactants based on alkylene diamine and evaluation of their corrosion inhibition efficiency on carbon steel in formation water, Egypt. J. Petrol. 26 (2017) 41-51.
[21] P. Geerlings, F. De Proft, W. Langenaeker, Conceptual density functional theory, Chem. Rev. 103 (2003) 1793-1874.
[22] R. G. Parr, R. G. Pearson, Absolute hardness: companion parameter to absolute electronegativity, J. Am. Chem. Soc. 105 (1983) 7512-7516.
[23] L. Pauling, The nature of the chemical bond, Cornell University Press, Ithaca, New York (January1960).
[24] A. Y. Musa, A. A. H. Kadhum, A. B. Mohamed, M. S. Takriff, Molecular dynamics and quantum chemical calculation studies on 4,4-dimethyl-3-thiosemicarbazide as corrosion inhibitor in 2.5 M H2SO4, Mater, Chem. Phys. 129 (2011) 660-665.
[25] K. C. Rani, R. Rimaharinastiti, E. Hendradi, Prepration and evaluation of ciprofloxacin implants using bovine hydroxyapatite-chitosan composite and glutarldhyde for osteomyelitis, Inter. J. Pharm. Pharm. Sci. 8 (2016) 45-51.
[26] F. Dufrasne, M. Gelbcke, J. Nève, ^{1}H-nuclear magnetic resonance determination of the enantiomeric purity of aliphatic primary amines, β-aminoalcohols, β-diamines and α-amino-acids with 1R-(-)-myrtenal: scope and limitations, Spectrochim. Acta A. Mol. Biomol. Spectrosc. 59 (2003) 1239-1245.
[27] T. Xiang, Synthesis and characterization of polymeric Schiff bases from 2,5-diformylfuran,"M. Sc. thesis, The Graduate Faculty of The University of Akron (December 2012).
[28] M. A. Quraishi, J. Rawat, M. jmal, Dithiobiurets: a novel class of acid corrosion inhibitors for mild steel, J. Appl. Electrochem. 30 (2000) 745-751.
[29] D. P. Schweinsberg, G. A. George, A. K. Nanayakkara, D. A.Steiner, The protective action of epoxy resins and curing agents—inhibitive effects on the aqueous acid corrosion firon and steel. Corros. Sci. 28 (1988) 33-42.
[30] A. K. Singh, M. A.Quraishi, Effect ofCefazolin on thecorrosionof mild steel in HCl solution,Corros. Sci. 52 (2010) 152-160.
[31] R. S. Abd El-Hameed, Aminolysis of polyethylene terephthalate waste as corrosion inhibitor for carbon steel in HCl corrosive medium, Adv. Appl. Sci. Res. 2 (2011) 483-499.
[32] M. H. Hussein, M. F. El-Hady, H. A. Shehata, M. A. Hegazy, H. H. Hefni, Preparation of some eco-friendly corrosion inhibitors having antibacterial activity from sea food waste, J. Surf. Deter. 16 (2013) 233–242.
[33] C. Verma, J. Haque, M. A. Quraishi, E.E. Ebenso, Aqueous phase environmental friendly organic corrosion inhibitors derived from one step multicomponent reactions: A review, J. Mol. Liq. 275 (2019) 18–40.
[34] R. Ravichandran, S. Nanjundan, N. Rajendran, Effect of benzotriazole derivatives on the corrosion of brass in NaCl solutions, Appl. Surf. Sci. 236 (2004) 241-250.
[35] W. I. Eldougdoug, A. I. Ali, A. Elaraby, E. M. Mabrouk, Corrosion inhibition of tri-cationic surfactant on carbon steel in hydrochloric acid solution, J. Basic Environ. Sci. 5 (2018) 289-300.

[36] R. S. Abd El-Hameed, Aminolysis of polyethylene terephthalate waste as corrosion inhibitor for carbon steel inHCl corrosive medium, Adv. Appl. Sci. Res. 2 (2011) 483-499.
[37] K. C. Emregül, M. Hayvalí, Studies on the effect of a newly synthesized Schiff base compound from phenazone and vanillin on the corrosion of steel in 2 M HCl, Corros. Sci. 48 (2006) 797-812.
[38] S. T. Keera, N. A. Negm, S. M. Ahmed, A. M. Badawi, Surface parameters and corrosion inhibition of some isothiouranium derivatives, J. Sci. Ind. Res. 61 (2002) 712-718.
[39] R. Govindasamy, S. Ayappan, Study of corrosion inhibition properties of novel semicarbazones on mild steel in acidic solutions, J. Chil. Chem. Soc. 60 (2015) 2786-2798.
[40] A. S. Patel, V. A. Panchal, N. K. Shah, Electrochemical impedance study on the corrosion of AI-pure in hydrochloric acid solution using Schiff base, Bull. Mater. Sci. 35 (2012) 283-290.
[41] R. P. Venkatesh, B. J. Cho, S. Ramanathan, J. G. Park, Electrochemical Impedance Spectroscopy (EIS) Analysis of BTA Removal by TMAH during Post Cu CMP Cleaning Process, J. Electrochem. Soc. 159 (2012) 447-452.
[42] A. M. Fenelon, C. B. Breslin, An electrochemical study of the formation of benzotriazole surface films on copper, zinc and a copper-zinc alloy, J. Appl. Electrochem.31 (2001) 509-516.
[43] H. Ma, X. Cheng, G. Li, S. Chen, Z. Quan, S. Zhao, L. Niu, The influence of hydrogen sulfide on corrosion of iron under different conditions. Corros. Sci. 42 (2000) 1669-1683.
[44] P. Kannan, P. Jithinraj, M. Natesan, Multiphasic inhibition of mild steel corrosion in H2S gas environment, Arab. J. Chem. 11 (2018) 388-404.
[45] M. A. Amin, Weight loss, polarization, electrochemical impedance spectroscopy, SEM and EDX studies of the corrosion inhibition of copper in aerated NaCl solutions, J. Appl. Electrochem.36 (2006) 215-226.
[46] M. O. Nkiko, A. Oluwabi, S. A. Ahmed, J. T. Bamgbose, Experimental and quantum chemical studies of the inhibition of copper with sodium dodecyl sulphate (SDS) in acidic medium, Engineering 10 (2018) 851-862.
[47] C. G. Zhan, J. A. Nichols, D. A. Dixon, Ionization potential, electron affinity, electronegativity, hardness, and electron excitation energy: molecular properties from density functional theory orbital energies, J. Phys. Chem. A. 107 (2003) 4184–4195.
[48] E. E. Ebenso, T. Arslan, K. Kandem, I. Love, C. Retlr, M. S. Lu, S. A. Umoren, Theoretical studies of some sulphonamides as corrosion inhibitors for mild steel in acidic medium, Inter. J. Quantum Chem. 110 (2010) 2614–2636.
[49] K. F. Khaled, Molecular simulation, quantum chemical calculations and electro-chemical studies for inhibition of mild steel by triazoles, Electrochim. Acta 53 (2008) 3484–3492.
[50] A. M. Al-Sabagh, N. M. Nasser, A. A. Farag, M. A. Migahed, A. M. F. Eissa, T. Mahmoud, Structure effect of some amine derivatives on corrosion inhibition efficiency for carbon steel in acidic media using electrochemical and quantum theory methods, Egypt. J. Petrol. 22 (2013) 101-116.
[51] A. Bendjeddou, T. Abbaz, S. Drissi, A. Gouasmia, D. Villemin, Quantum chemical studies on molecular structure and reactivity descriptors of a series of trimethyltetrathiafulvalene functionalized by conjugated substituent, J. Adv. Chem. Sci. 2 (2016) 318–32.